energies

MDPI

Article

Data-Driven Energy Consumption Analysis and Prediction of Real-World Electric Vehicles at Low Temperatures: A Case Study Under Dynamic Driving Cycles

Yifei Zhao [1], Hang Liu [2], Jinsong Li [1], Hongli Liu [3,*] and Bin Li [3,*]

[1] School of Mechanical and Electrical Engineering, Hainan University, Haikou 570228, China
[2] CATARC Automotive Test Center Co., Ltd., Changzhou 213100, China
[3] School of Automobile, Chang'an University, Xi'an 710018, China
* Correspondence: hongli_liu_lhl@chd.edu.cn (H.L.); binli@chd.edu.cn (B.L.)

Abstract: Accurate analysis and prediction of low-temperature energy consumption in pure electric vehicles can provide a reliable reference for energy optimization strategies, thereby alleviating range anxiety. Here, we propose a data-driven energy consumption analysis and prediction approach for real-world electric vehicles in cold conditions. Specifically, the dataset was divided into multiple kinematic segments by the fixed-step intercept method, and principal component analysis was applied on segment parameters, showing the average speed and acceleration time had the greatest impact on energy consumption at −7 °C. Then, a Bayesian optimized XGBoost model, with the two factors above as input, was constructed to predict the cumulative driving and total energy consumption. This method was validated with two different types of pure electric vehicles under different dynamic driving cycles. The results demonstrated that the model could predict low-temperature energy consumption accurately, with all mean relative errors less than 3%.

Keywords: electric vehicle; low temperature; energy consumption prediction; machine learning; Bayesian optimization

Academic Editor: Felix Barreras

Received: 14 January 2025
Revised: 16 February 2025
Accepted: 27 February 2025
Published: 3 March 2025

Citation: Zhao, Y.; Liu, H.; Li, J.; Liu, H.; Li, B. Data-Driven Energy Consumption Analysis and Prediction of Real-World Electric Vehicles at Low Temperatures: A Case Study Under Dynamic Driving Cycles. *Energies* **2025**, *18*, 1239. https://doi.org/10.3390/en18051239

1. Introduction

As the global energy crisis and environmental issues intensify, the automotive industry is actively transitioning toward more sustainable and environment-friendly solutions. Pure electric vehicles (EVs) have attracted significant attention and promotion in the market as a new type of emission-free, high-efficiency transportation option [1,2]. While EVs offer notable energy saving and emissions reductions, their performance in cold climates is severely impacted by increased energy consumption and reduced range performance at low temperatures [3]. This surge in energy consumption in cold regions may force the power system to rely on fossil energy peaking, indirectly undermining the carbon-reducing benefits of electrification. In addition, range anxiety due to low temperatures may slow down the electrification process in cold regions, exacerbating the spatial imbalance in global transportation emission reduction targets. To avoid such problems and enhance the applications of EVs in cold areas, it is of great importance to analyze and predict the energy consumption (EC) of EVs at low temperatures, achieving optimal energy management to reduce unnecessary energy consumption.

Up to now, some studies have been carried out to analyze the potential effects of various factors on the EC of EVs. For example, Wang et al. studied the EC characteristics of EVs at a high speed levels through a power analyzer and chassis dynamometer, studying

on the DC power consumption of vehicles under the latest Chinese Light-Duty vehicle Test Cycle [4]. Based on real-road driving data of EVs, Zhao et al. analyzed the influence of driving status on the EC from the perspective of speed and acceleration in a comprehensive way [5]. Chen et al. established a simulation model of vehicle energy flow to analyze the EC characteristics of each vehicle component, as well as the energy-flow decomposition under different driving cycles and different temperatures, suggesting that energy management optimization for pure electric vehicles should pay more attention to the mechanical transmission, air conditioning system, and controlling strategy of the electric driving system [6]. Zhao et al. further researched the influence of driving style on the EC of EVs under an integrated driving cycle according to the direction of energy flow under a constant driving speed [7]. Yang et al. tried to analyze the influence of different seasonal temperatures and different driving habits on EV EC from one-year real-road driving data [8]. Iora and Triboli established an EC estimation model based on the driving data of a Nissan Leaf electric vehicle and evaluated the influence of ambient temperature on the vehicle EC [9]. Xie et al. analyzed the influence of different environmental and control parameters on the total EC with the help of an EV simulation model in single-pedal mode and found that the main factors influencing energy consumption and driving range were average vehicle speed, running time, and the frequency distribution of the braking process [10]. Berzi et al. adopted intelligent management of onboard loads to smooth the EV EC due to auxiliary systems, especially for the HVAC (heating, ventilation, and air conditioning) system [11]. EC-relative factors such as vehicle speed, acceleration, ambient temperature, etc. have been used as inputs to various EC prediction models, and how to fully utilize them to enhance the accuracy of these models has also become a major concern for the automotive industry in recent years.

To reduce prediction errors, scholars have made great efforts to propose some effective solutions that achieve satisfying performance in particular conditions. Wang et al. established a model to predict the total EC based on real-road collected EV data, combining the multiple linear regression and RBF neural network methods. The results showed that the prediction accuracy of the combined model was significantly higher than that of a single multiple regression model [12]. Cao et al. realized an accurate EC prediction by mining driving behavior information through a big-data model with large sampling intervals, which consisted of various trajectory data from drivers [13]. Zhong et al. proposed a deep learning method to predict the trip EC of EVs, fusing the state information of the vehicle itself and traffic network features to train the deep neural network [14]. Sarrafan et al. improved the estimation model for EV EC by integrating environmental conditions and driving efficiency. The prediction error between the estimated and measured values was less than 0.5% [15]. Miri et al. used MATLAB/Simulink to establish a BMW i3 vehicle model that contained the powertrain, battery system, driver system, regenerative braking, and auxiliary devices to estimate the EC; the model's prediction error was around 2–6% [16]. Wang et al. also built a model based on a certain EV type for EC prediction, including the road load, power system, regenerative braking, auxiliary system, and battery system. Its maximum prediction error was only 5% [17].

However, few of the aforementioned studies have paid enough attention to the prediction of low-temperature energy consumption (EC), which is quite difficult because of the interference of ambient temperature and the air-conditioning system. Furthermore, the procedures by which these studies have selected EC-relative factors have been relatively complicated. To bridge the aforementioned research gaps, we propose a Bayesian optimized XGBoost model based on easily selected but effective factors to accurately predict the low-temperature driving and total EC of EVs. The main contributions of our study can be summarized as:

(1) Selecting highly relevant factors in a rather brief way. Average speed and acceleration time were selected by principal component analysis and presented major impacts on the EC of EVs at −7 °C, leading to regular changes in EC while they were increasing. Factors changed when the environment became much cooler, but they were still efficient.
(2) Establishing a prediction model to realize an accurate EC prediction at low temperatures. High accuracy was witnessed in the prediction of driving EC, and accuracy decreased only slightly when predicting the total EC.
(3) Validating the method with dynamic driving cycles. Real-world vehicle data were collected under effective driving cycles that included various working conditions. Thus, low-temperature EC could be analyzed and predicted on a much more reliable basis.

2. Experimental

In this study, two pure electric vehicles were selected as test vehicles, as shown in Figure 1a,b. Here, car W stands for the white vehicle, and car B stands for the black one. During the test, the brake recovery function was turned on, and the ECO mode was selected as the driving mode. Specifically, the top two pictures of Figure 1a show the real experimental scenario, and the bottom one shows a schematic of each component in the test: the vehicle, environment chamber, auxiliary screen, head-on fan, chassis dynamometer, power analyzer, etc. The environment chamber could simulate the temperature, humidity, and sunshine under various climatic conditions. It provided a low-temperature environment of −7 °C for car W and another one of 15 °C for car B. In practice, this temperature range was wide enough to evaluate the EC and driving range of the EVs under cold climate conditions. The auxiliary screen was loaded with dynamic cycles to assist the driver in driving in accordance with the test requirements. The head-on fan adjusted the wind speed to follow changes in velocity, providing realistic cooling for the vehicle motor. The chassis dynamometer simulated the actual driving resistance on the road and recorded the vehicle speed during the test. The power analyzer collected relevant electrical parameters of the test vehicle; its type and sampling frequency were HIOKI PW3390 (HIOKI, Shanghai, China) and 1 Hz, respectively, as shown in the bottom half of Figure 1a. This power analyzer could achieve a high-level power accuracy of ±0.04% rdg and ±0.05% f.s. It maintained stable amplitude and phase accuracy at high frequency and acquired up to 8 channels of data synchronously. Electrical parameters collected included current and voltage of the 12 V battery, drive motor, PTC, DCDC, etc.; a sample of data acquisition is presented in Figure 1c.

The main procedure of the test is shown in Figure 1d. The vehicle first coasted to determine the loading coefficient of the chassis dynamometer resistance, and the environment resistance coefficient was set as 1.1 times larger than that in the normal temperature. After the discharge and recharge stage, the vehicle was put in the cold environment for a long time, and the test then began. During the test, the necessary data were collected.

In particular, the auxiliary screen loaded the newest cycle in China for car W, which was proposed in the China national standard GB/T 18386.1-2021 "Test Methods for Energy Consumption and Driving Range of Electric Vehicles Part 1: Light Duty Vehicles" (CLTC-P) [18], as shown in Figure 2a. For car B, the auxiliary screen loaded a common interurban cycle shown in Figure 2b.

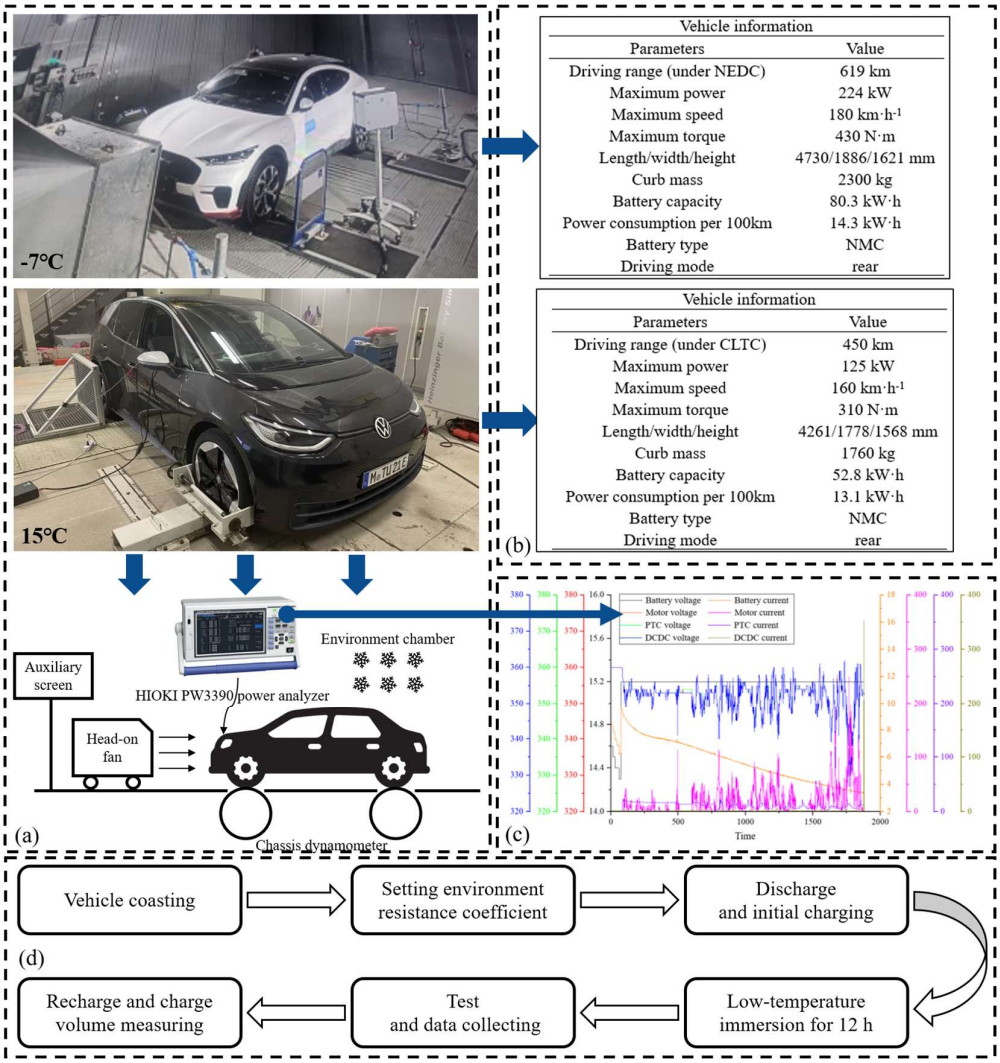

Figure 1. (**a**) The experimental platform for proposed low-temperature test, (**b**) the vehicle technical information, (**c**) the sample data from the power analyzer, and (**d**) the procedure of the test.

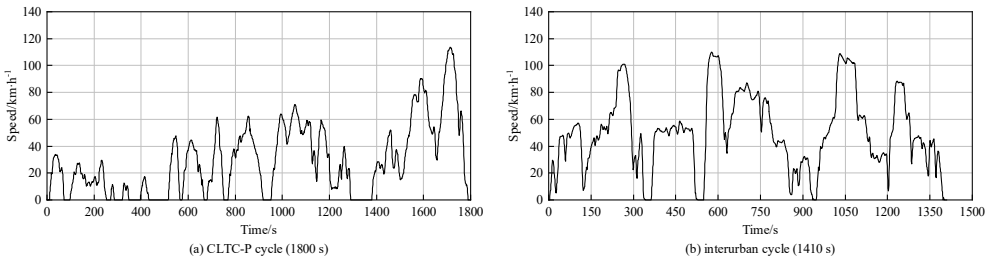

Figure 2. (**a**) The CLTC-P driving cycle and (**b**) the common interurban cycle.

Besides these, a pretest for car W, in which the vehicle ran only 3 CLTC-P cycles to collect more data on the warm-up process, was carried out before the formal test. In the formal test, car W ran 23 CLTC-P cycles, and car B ran 23 interurban cycles, until their batteries are almost completely depleted.

3. Analysis of EC at Low Temperatures

The total EC is greatly affected by particular road environments, and its deterioration intensifies greatly at low temperatures [19], which makes prediction thereof less accurate. This study first analyzed the effects of different characteristic parameters on the low-

temperature EC of EVs and selected valuable ones in a rather brief way. To avoid repeated descriptions, the following content focuses mainly on car W.

3.1. Analysis of Low-Temperature Energy Flow

The battery power is consumed mainly by the drive motor, PTC (positive temperature coefficient heaters), and DCDC (DC–DC converter) when in cold conditions. The drive motor overcomes the driving resistance to keep the vehicle moving in accordance with the will of the driver, the PTC provides enough heat in the low-temperature environment to avoid extreme coldness, and the DCDC converts the original DC voltage into a larger or smaller one, during which energy is continually consumed. As for the recharge of battery power, besides long-time charging, the battery power recovers mainly by the recycled energy from the regenerative braking system. Thus, EV battery energy flow in cold environments is:

$$E_b + E_r = E_{motor} + E_{ptc} + E_{DCDC} \quad (1)$$

where E_b is the output power of the power battery, kW·h; E_r is the input power of braking recovery, kW·h; E_{motor} is the power consumed by the drive motor, kW·h; E_{ptc} is the power consumed by the PTC, kW·h; and E_{DCDC} is the power consumed by the DCDC, kW·h.

3.2. Kinematic Segments Division

Dynamic driving cycles can not only provide a reference for the power system design of traditional fuel vehicles to achieve the effects of fuel saving and emission reduction but optimize the power and energy storage systems for EVs to reduce the EC and increase driving mileage through a reasonable distribution of energy flow. These cycles are mainly speed–time curves containing many kinematic segments.

To analyze the EC of EVs, this study adopted the fixed-step interception method [20] to divide the data into a number of short kinematic segments with a fixed time interval of 60 s (50 s for car B); 780 kinematic segments were obtained in total after this process (644 segments from car B). According to the literature [21], 15 characteristic parameters were selected to describe each kinematic segment, as shown in Table 1, which also presents some samples of segment characteristic parameters. It is obvious that there were significant differences in characteristic parameters between different kinematic segments.

Table 1. Characteristic parameters of kinematic segments and some samples from car W.

Number	Symbol	Name	Unit	1	2	3	4	5	...	779	780
1	V_m	Average speed	km·h^{-1}	21.21	8.29	18.73	17.39	3.38	...	100.57	33.39
2	V_{max}	Maximum speed	km·h^{-1}	33.62	23.62	27.37	29.63	18.21	...	114.22	76.48
3	V_s	Standard deviation of speed	km·h^{-1}	11.91	8.68	5.3	6.23	4.52	...	11.49	26.89
4	A_m	Average acceleration	m·s^{-2}	1.37	1.25	0.57	1.02	1.29	...	1.31	2.73
5	D_m	Average deceleration	m·s^{-2}	3.28	2.47	1.37	3.26	2.9	...	2.78	3.97
6	A_{max}	Maximum acceleration	m·s^{-2}	−0.73	−1.62	−0.83	−0.84	−1.44	...	−1.5	−2.39
7	D_{max}	Maximum deceleration	m·s^{-2}	−1.5	−3.58	−1.29	−3.03	−3.18	...	−5.07	−6.97
8	T_i	Idle time	s	29	20	28	32	10	...	30	9
9	T_a	Acceleration time	s	21	16	30	26	20	...	29	40
10	T_d	Deceleration time	s	9	23	0	0	29	...	0	10
11	T_c	Uniform speed time	s	1	1	2	2	1	...	1	1
12	P_i	Ratio of idle time		0.48	0.33	0.47	0.53	0.17	...	0.5	0.15
13	P_a	Ratio of acceleration time		0.35	0.27	0.5	0.44	0.33	...	0.48	0.66
14	P_d	Ratio of deceleration time		0.15	0.38	0	0	0.48	...	0	0.17
15	P_c	Ratio of uniform speed time		0.02	0.02	0.03	0.03	0.02	...	0.02	0.02

3.3. Principal Component Analysis

The high dimensionality of the characteristic parameters and the large correlation between them would interfere with the analyzing and calculating processes. Therefore, the 15 characteristic parameters needed to be subjected to principal component analysis, which

is a commonly used dimensionality-reduction technique to convert high-dimensional variables into low-dimensional variables. According to the principles of principal component analysis [22], the number of principal components is determined based on the cumulative contribution rate, which should be greater than 85% (86.61% for car W, as shown in Table 2; 86.01% for car B).

Table 2. Cumulative contribution rates of principal components.

Principal Component	Variance	Percentage of Variance/%	Cumulative Contribution Rate/%
1	5.21	34.70	34.70
2	3.51	23.38	58.08
3	2.41	16.07	74.15
4	1.87	12.46	86.61
5	0.92	6.16	92.77
6	0.54	3.62	96.39
7	0.35	2.34	98.73
8	0.11	0.75	99.48
9	0.06	0.41	99.89
10	0.02	0.11	100.00

The key characteristic parameters were determined according to the principal component loading matrix in Figure 3a. The first principal component represents average speed and maximum speed; the second principal component represents acceleration time and the ratio of acceleration time; the third principal component represents the standard deviation of speed and average acceleration; the fourth principal component represents uniform speed time and the ratio of uniform speed time. To simplify the model inputs, the average speed and acceleration time were selected as the final parameters for each segment in our study. As for car B, average speed and deceleration time were selected according to Figure 3b.

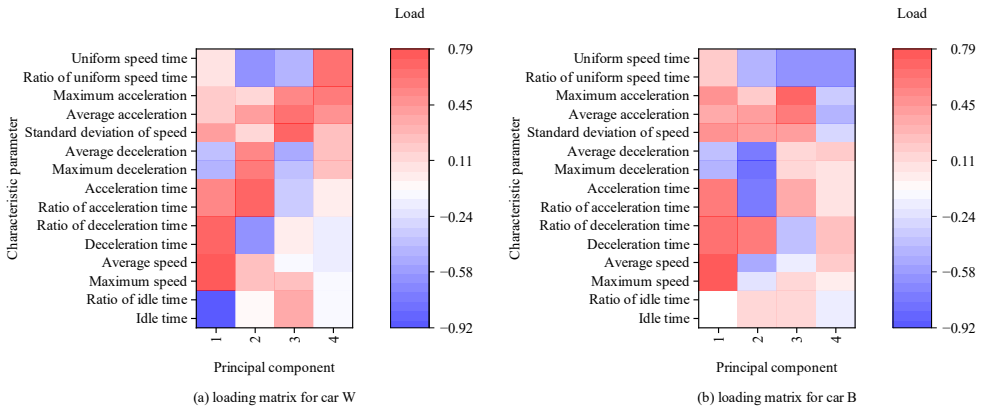

Figure 3. (**a**) The principal component matrix for car W and (**b**) the matrix for car B.

3.4. Analysis of Segment EC

In this paper, total EC means the total energy consumption of the vehicle, including all the consumption of components in the vehicle, and the driving EC refers only to consumption from the drive motor itself. Because of the test arrangement, only the total EC data of car B were collected.

According to the results of the principal component analysis above, this study analyzed the effect of average speed and acceleration time on the segment EC. Figure 4a shows the variation of the segment total EC with average speed, the scatters fitted with a quadratic

term. It can be seen that there was a trend of EC decreasing and then increasing with increasing average speed. When the average speed was in the interval of 0–20 km·h^{-1}, the distribution of the EC is much higher and more dispersed, with the average EC achieving 646.57 Wh·(km)$^{-1}$. As the average speed increased and reached the economic interval of 20–60 km·h^{-1}, the EC reached its lowest level, only 204.83 Wh·(km)$^{-1}$. On average, the EC was 3.16 times larger at low-speed intervals than in the medium-speed intervals. This phenomenon was due mainly to the increased time of drive motor operation in the low-efficiency zone and the greater EC from the low-temperature air-conditioning system at the initial stages.

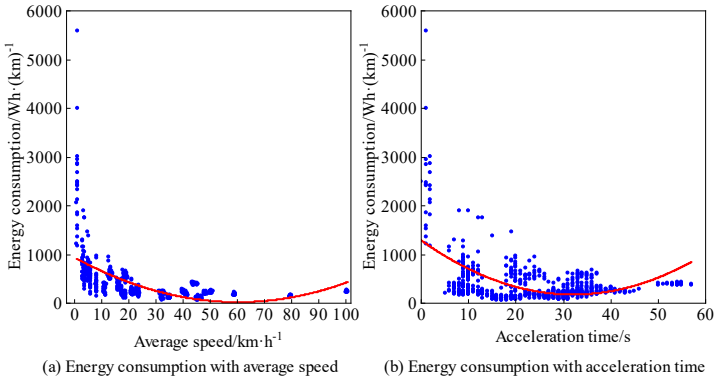

Figure 4. Each blue point represents a segment, and the red curves are quadratic fits to the energy consumption of all segments. (**a**) The energy consumption curve with the average speed and (**b**) the energy consumption curve with acceleration time.

Figure 4b shows the variation of EC with acceleration time, the scatters also fitted with a quadratic term. It is obvious that the EC trend was similar to that with average speed. The reasons are as follows: when the acceleration time is short, the road traffic is congested, thus being equal to the condition of low average speed; when the acceleration time is appropriately extended, the vehicle operates for more time in the economic zone with the lowest EC; as the acceleration time is extended again and the vehicle reaches a high speed, the EC increases cause the motor to leave the optimal working point, and the air resistance increases significantly, which forces the motor to run under a high load.

Similarly, Figure 5 shows the variation of EC with average speed and acceleration time. The trends in Figure 5 were slightly different from those in Figure 4, mainly because of the different cycle and the cooler temperature.

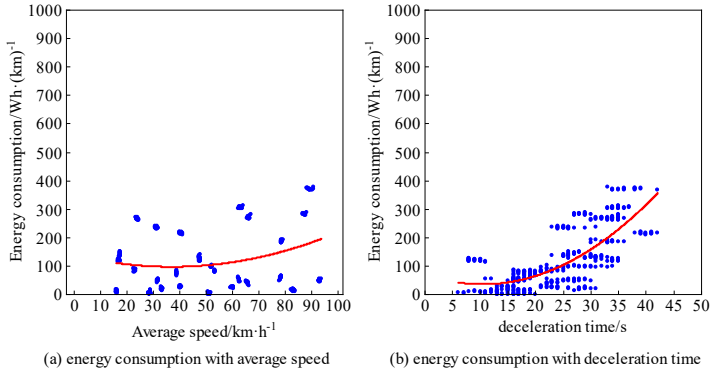

Figure 5. Each blue point represents a segment, and the red curves are quadratic fits to the energy consumption of all segments. (**a**) The energy consumption curve with the average speed and (**b**) the energy consumption curve with deceleration time.

The average speed and acceleration time were selected as the inputs for K-means clustering. This algorithm is a commonly used data analysis method that divides the datapoints into K clusters by constantly updating the mass centers and redistributing the data through an iterative optimization algorithm, finally finding a solution that minimizes the objective function [23]. The expectation of clustering is to make the total sum of squared errors from each sample point to its nearest clustering center as small as possible. The spatial distance from the sample point to its clustering center is:

$$d(x, C_i) = \sqrt{\sum_{j=1}^{m} (x_j - C_{ij})^2} \tag{2}$$

where x is the dataset; C_i is the i-th clustering center; m is the data dimension; and x_j, C_{ij} are the j-th parameters of x, C_i.

The sum of squared error S for the dataset is calculated as:

$$S = \sum_{i=1}^{k} \sum_{x \in C_i} |d(x, C_i)|^2 \tag{3}$$

where k is the number of clustering categories. The smaller the sum of squared error, the better the clustering results.

The number of clustering categories k is determined according to the elbow method. The point where the steep declining trend in the sum of squared error begins to slow down is called the "elbow inflection point", and there is no longer a significant decrease in the sum of squared error with increasing numbers of clustering categories after this point (here, k was selected as 4, as shown in Figure 6).

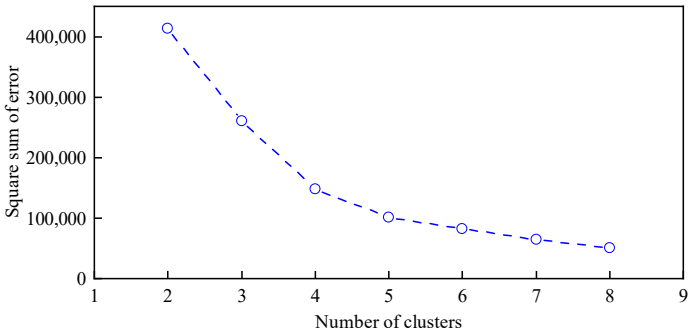

Figure 6. Curve of the elbow method.

After the K-means clustering, the kinematic segments were divided into four different classes. Figure 7 shows the distribution of segment total EC in these four conditions. For red points under working condition 1, its segment EC was more unstable and had a large degree of dispersion, which was due mainly to the low speed and inefficient running motor, and its average EC (750.09 Wh·(km)$^{-1}$) was 3.92 times higher than that of yellow points under working condition 3 (191.45 Wh·(km)$^{-1}$). With increasing average speed and acceleration time, the EC of different conditions tended to stabilize, like the trend in Figure 4.

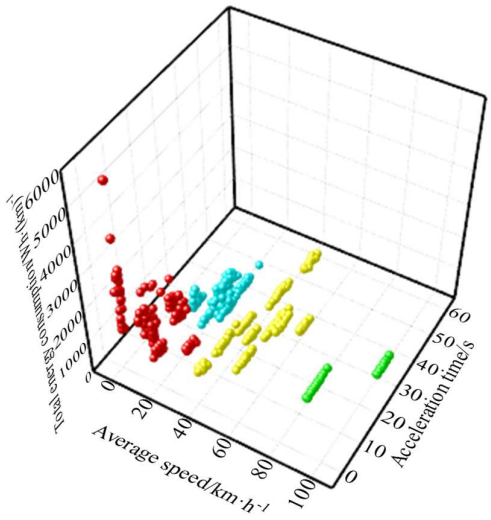

Figure 7. Visualization of clustering results. The title of *z*-axis is "total energy consumption/Wh·(km)$^{-1}$". Red points represent the segment EC under working condition 1, blue points under condition 2, yellow points under conditon 3 and green points under condition 4.

4. Prediction of EC at Low Temperature

4.1. Model Introduction

After the preselection of sufficient characteristic parameters, the first two principal components with the highest interpretability were identified through the PCA loading matrix. Each principal component mainly reflected a key characteristic parameter (key factor). Finally, the two key factors were used as the input features to predict the segment EC (for car W, these were segment average speed and segment acceleration time; for car B, they were segment average speed and segment deceleration time).

This study established the XGBoost model to predict the driving and total EC of kinematic segments. XGBoost is a powerful machine learning algorithm that is used mainly for prediction and classification through parametric regression [24]. Compared with the random forest method, XGBoost has better accuracy and speed on medium-sized datasets (sample size 10^3~10^6) and avoids the overfitting phenomenon, which is prone to occur in neural networks such as LSTM by L1 and L2 regularization. With lower deployment and computation costs, it can achieve a good balance between accuracy and efficiency.

The objective function of XGBoost consists of two parts: the loss function and the regularization term. The former measures the model prediction error, and the latter controls the model complexity as well as preventing overfitting. The exact form of the objective function depends on the problem being researched. For regression prediction, the loss function is usually the mean square error:

$$\mathcal{L} = 1/2 \sum (y_i - \overline{y}_i)^2 \tag{4}$$

where $\mathcal{L}$ is the objective function, y_i is the true target value, and $\bar{y}_i$ is the predicted value.

The regularization term includes L1 regularization and L2 regularization:

$$R = \lambda * \sum w^2 \tag{5}$$

where R is the regularization term, λ is the regularization parameter and controls the regularization intensity, and w is the weight parameter.

However, the single XGBoost model is susceptible to falling into local optimal solutions because of improper initial selection of hyperparameters. The improved Bayesian optimized XGBoost model can avoid such problems, and it has high efficiency and robustness while

predicting; it can find the near-optimal hyperparameter configuration with a small number of objective function evaluations [25]. Therefore, it was selected as the EC prediction model in this study. Here, the search space of Bayesian optimization was: max_depth in (3, 7), learning rate in (0.01, 0.3), n_estimators in (50, 500), gamma in (0, 1), min_child_weight in (1, 10). The iterations were set as 30.

All kinematic segments under four different conditions were divided into a training set and a test set. Then, the training set was used to train the XGBoost model, the optimal hyperparameter configurations of which were obtained by Bayesian optimization. The test set was used to evaluate the prediction effects, with the mean squared error, root mean squared error (RMSE), mean absolute error, and R2 as evaluating indices.

4.2. Analysis of Prediction Results

Figure 8 shows the results of EC prediction. In Figure 8a, the predicted driving EC was in high agreement with the real values, but in Figure 8b,c, the predicted total EC was not as close to the real values the predicted driving EC was.

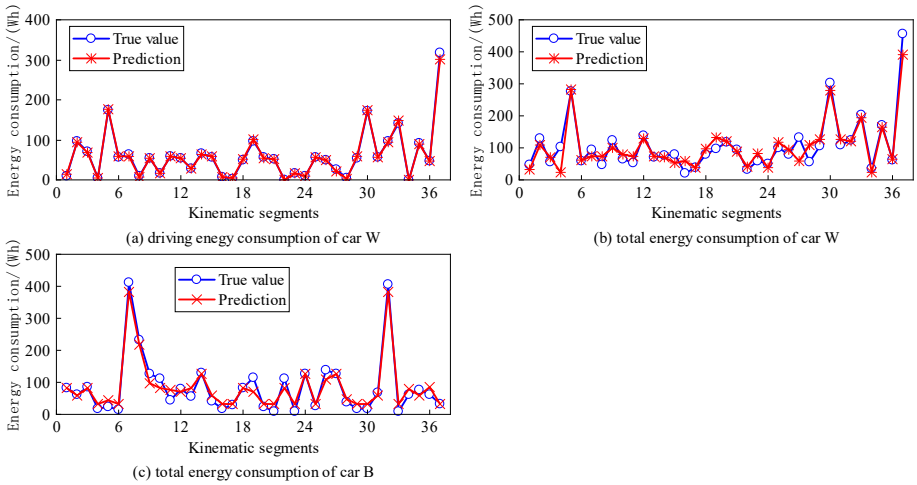

Figure 8. (**a**) Prediction results of the driving energy consumption of car W, (**b**) prediction results of the total energy consumption of car W, and (**c**) prediction results of total energy consumption of car B.

Table 3 presents the evaluation indices of the prediction results of both driving and total EC. It can be seen that the R^2 of all kinds of the EC was greater than 0.9, which indicates that the prediction results were all satisfying. However, the mean absolute error of the total EC was significantly higher than that of the driving EC. This was because the total EC in low-temperature environments was affected not only by the drive motor but by the EC of the PTC and DCDC, which reduced the prediction accuracy. However, with enough similar-traffic-environment segments in the interurban cycle, the accuracy of total EC prediction decreased in car B, meaning the model would improve with more valid data.

Table 3. Evaluation indices of prediction results.

Vehicle	Energy Consumption	RMSE/Wh	R^2	Mean Absolute Error/Wh	Mean Relative Error/%
Car W	Driving	9.86	0.9874	5.02	0.25
Car W	Total	24.20	0.9069	17.56	2.38
Car B	Total	28.08	0.9092	13.65	1.47

Based on the prediction results of driving and total EC of all kinematic segments, the cumulative EC of the whole test process was further analyzed. As shown in Figure 9a,

predicted values of cumulative driving EC were always close to real values, but as shown in Figure 9b,c the predicted values of cumulative total EC were slightly smaller than the real values and had a larger deviation in the middle stage of the test.

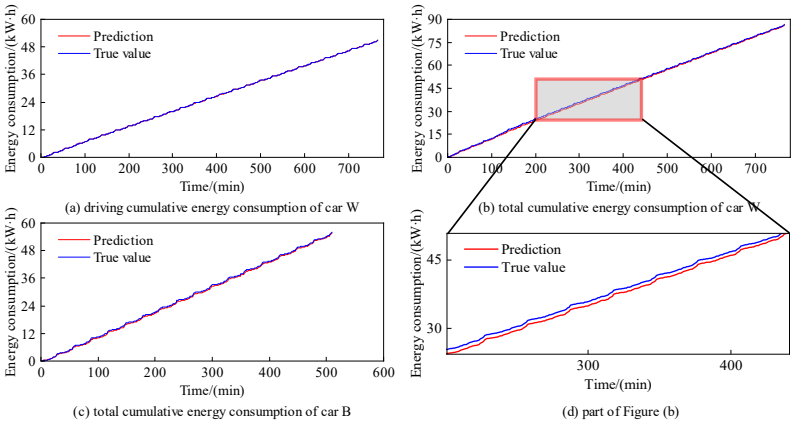

Figure 9. (**a**) Prediction results of the cumulative driving energy consumption of car W, (**b**) the cumulative total energy consumption of car W, and (**c**) the cumulative total energy consumption of car B; (**d**) an enlarged part of the cumulative total energy consumption prediction for car W.

Figure 10 shows the absolute and relative errors of prediction results. It indicates that when the energy demand stabilized, the total EC prediction could also reach a high accuracy easily. Meanwhile, the absolute errors of both driving and total EC had the same trend: increasing first and then decreasing. They increased at the initial stage because the vehicle is still cold while starting. At this time, the driving resistance is unstable, and the energy demand for warming the passenger compartment at low temperatures is urgent, resulting in an increase in the absolute error. With the stabilization of the power output from the drive and transmission systems, the temperature of the passenger compartment also rises more stably. Thus, the absolute error starts to decrease because of the constant energy demand. The relative errors also showed a trend of being larger at the beginning and gradually smaller with time. This was because there were fewer kinematic segments predicted at the beginning, and the real cumulative EC in the denominator was smaller.

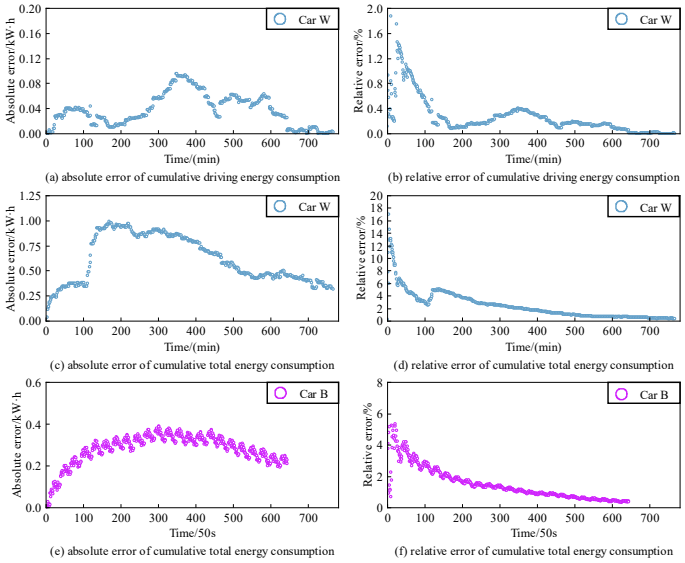

Figure 10. (**a**) Absolute error of cumulative driving energy consumption prediction from car W, (**b**) relative error of cumulative driving energy consumption prediction from car W, (**c**) absolute error

of cumulative total energy consumption prediction from car W, (**d**) relative error of cumulative total energy consumption prediction from car W, (**e**) absolute error of cumulative total energy consumption prediction from car B, and (**f**) relative error of cumulative total energy consumption prediction from car B.

5. Conclusions

This study proposes a data-driven method, aiming at selecting the most valuable factors impacting EV energy consumption at low temperatures and accurately predicting the EC under cold and dynamic driving conditions. The main conclusions are summarized as follows:

(1) Average speed and acceleration time were found to have notable impacts on EV energy consumption at −7 °C, and the segment energy consumption showed a trend of decreasing and then increasing with increasing average speed or acceleration time. This factor-selecting method was still valid under changes in cycle and temperature.
(2) High attention should be paid to the significantly consumed energy at low speed levels, and the optimization of EV energy flow under such conditions should be considered as a necessity in the stage of vehicle designing.
(3) Driving energy consumption at low temperatures was stable enough to achieve a high accuracy of prediction, while for the total energy consumption under such conditions, it was not easy to get satisfying results. However, with enough traffic data, the proposed Bayesian optimized XGBoost model based on these two factors could also show reliable prediction performance, with the mean relative error reaching 1.47%, as shown in the results for car B.
(4) The method proposed in this paper is applicable to various types of electric vehicles, such as cars or trucks. It can also be used to study and predict the trend of energy consumption of electric vehicles at other temperatures (for example, high-temperature environments), which has a wide range of application scenarios.

In this study, only two representative low temperatures were selected as test conditions, so the stability of energy consumption prediction at more temperatures will be investigated in our future work, which will also include more, different vehicle data. In addition, whether the method can realize a satisfying result with fast response, high accuracy, and low computing power consumption in a real-time prediction process will also be explored in our subsequent study.

Author Contributions: Conceptualization, Y.Z. and H.L. (Hang Liu); methodology, Y.Z.; software, H.L. (Hongli Liu); validation, Y.Z., H.L. (Hang Liu), B.L., and J.L.; formal analysis, H.L. (Hongli Liu); investigation, H.L. (Hang Liu); resources, Y.Z.; data curation, H.L. (Hongli Liu); writing—original draft preparation, Y.Z.; writing—review and editing, H.L. (Hang Liu), H.L. (Hongli Liu), B.L., and J.L.; visualization, J.L.; supervision, Y.Z., B.L., and J.L.; project administration, H.L. (Hang Liu); funding acquisition, B.L. All authors have read and agreed to the published version of the manuscript.

Funding: This research was supported by Research on the Innovation Chain of New Energy Vehicles in Xianyang City (L2023-RKX-SJ-035) and the Fundamental Research Funds for the Central Universities, CHD (300102223208).

Data Availability Statement: The raw data supporting the conclusions of this article will be made available by the authors on request.

Conflicts of Interest: Author Hang Liu was employed by the CATARC Automotive Test Center Co., Ltd. The remaining authors declare that the research was conducted in the absence of any commercial or financial relationships that could be construed as a potential conflict of interest.

References

1. Ke, W.; Zhang, S.; He, X.; Wu, Y.; Hao, J. Well-to-wheels energy consumption and emissions of electric vehicles: Mid-term implications from real-world features and air pollution control progress. *Appl. Energy* **2017**, *188*, 367–377. [CrossRef]
2. Zhang, R.; Hanaoka, T. Deployment of electric vehicles in China to meet the carbon neutral target by 2060: Provincial disparities in energy systems, CO_2 emissions, and cost effectiveness. *Resour. Conserv. Recycl.* **2021**, *170*, 105622. [CrossRef]
3. Ning, Q.; He, G.; Xiong, G.; Sun, W.; Song, H. Operation strategy and performance investigation of a high-efficiency multifunctional two-stage vapor compression heat pump air conditioning system for electric vehicles in severe cold regions. *Sustain. Energy Technol. Assess.* **2021**, *48*, 101617. [CrossRef]
4. Wang, Z.Y.; Sun, L.; Lei, L.G. Analysis of DC Energy Consumption of Pure Electric Vehicles under Two Test Methods. *Intern. Combust. Engine Accessories* **2021**, *11*, 68–69.
5. Zhao, J.Y. Electric Vehicle Energy Consumption Prediction and Analysis Based on Real-World Driving Data. Master's Thesis, Hebei University of Technology, Tianjin, China, 2022.
6. Chen, H.A. Energy Flow Simulation and Energy Consumption Analysis of Pure Electric Vehicles. Master's Thesis, Chongqing University of Technology, Chongqing, China, 2021.
7. Zhao, J.W.; Hu, M.H.; Rong, Z.B.; Fu, C.Y. Effect of Driving Style on the Energy Consumption of an Electric Vehicle. *J. Chongqing Univ.* **2021**, *44*, 103–115.
8. Yang, D.; Liu, H.; Li, M.; Xu, H. Data-driven analysis of battery electric vehicle energy consumption under real-world temperature conditions. *J. Energy Storage* **2023**, *72*, 108590. [CrossRef]
9. Iora, P.; Tribioli, L. Effect of Ambient Temperature on Electric Vehicles' Energy Consumption and Range: Model Definition and Sensitivity Analysis Based on Nissan Leaf Data. *World Electr. Veh. J.* **2019**, *10*, 2. [CrossRef]
10. Xie, Y.; Li, Y.; Zhao, Z.; Dong, H.; Wang, S.; Liu, J.; Guan, J.; Duan, X. Microsimulation of electric vehicle energy consumption and driving range. *Appl. Energy* **2020**, *267*, 115081. [CrossRef]
11. Berzi, L.; Delichristov, D.; Favilli, T.; Pierini, M.; Ponchant, M.; Qehajaj, A.; Pugi, L. Smart Energy Management of Auxiliary Load for Electric Vehicles. In Proceedings of the 2020 20th IEEE International Conference on Environment and Electrical Engineering and 2020 4th IEEE Industrial and Commercial Power Systems Europe (EEEIC/I&CPS Europe), Madrid, Spain, 9–12 June 2020.
12. Wang, X.D. Energy Consumption Prediction of Electric Vehicles Based on Combination Model. Master's Thesis, Dalian University of Technology, Dalian, China, 2021.
13. Cao, F.B. Driving Style Analysis and Energy Consumption Prediction of New Energy Buses Based on Driving Data. Master's Thesis, Huazhong University of Science & Technology, Wuhan, China, 2021.
14. Zhong, Z.Y. The Prediction of Travel Energy Consumption of Electric Vehicle with Traffic Information. Master's Thesis, Beijing Institute of Technology, Beijing, China, 2017.
15. Sarrafan, K.; Sutanto, D.; Muttaqi, K.M.; Town, G. Accurate range estimation for an electric vehicle including changing environmental conditions and traction system efficiency. *IET Electr. Syst. Transp.* **2017**, *7*, 117–124. [CrossRef]
16. Miri, I.; Fotouhi, A.; Ewin, N. Electric vehicle energy consumption modelling and estimation-A case study. *Int. J. Energy Res.* **2021**, *45*, 501–520. [CrossRef]
17. Wang, J.J.; Besselink, I.I.; Nijmeijer, H. Battery electric vehicle energy consumption modelling for range estimation. *Int. J. Electr. Hybrid Veh.* **2017**, *9*, 79–102. [CrossRef]
18. *GB/T 18386.1-2021*; Test Methods for Energy Consumption and Driving Range of Electric Vehicles Part 1: Light Duty Vehicles. Standards Press of China: Beijing, China, 2021.
19. Wang, W.W.; Sun, F.C. Key Technologies and Prospects of All-Climate New Energy Vehicles. *Strateg. Study CAE* **2019**, *21*, 47–55. [CrossRef]
20. Hu, Z.Y. Study on Construction Method of Urban Driving Cycle of Passenger Vehicles. *J. Highw. Transp. Res. Dev.* **2019**, *36*, 142–150.
21. Li, B. Research on Energy Management Strategy of Fuel Cell Vehicle Based on Driving Condition Prediction. Master's Thesis, Jilin University, Changchun, China, 2021.
22. Azadeh, A.; Nasirian, B.; Salehi, V.; Kouzehchi, H. Integration of PCA and DEA for identifying and improving the impact of Six Sigma implementation on job characteristics in an automotive industry. *Qual. Eng.* **2017**, *29*, 273–290. [CrossRef]
23. Luo, J.J. Research and Application of Vehicle Driving Condition Construction Method in Complex Environment. Master's Thesis, Nanjing University of Science & Technology, Nanjing, China, 2021.

24. Asselman, A.; Khaldi, M.; Aammou, S. Enhancing the prediction of student performance based on the machine learning XGBoost algorithm. *Interact. Learn. Environ.* **2023**, *31*, 3360–3379. [CrossRef]
25. Yin, J.; Li, N. Ensemble learning models with a Bayesian optimization algorithm for mineral prospectivity mapping. *Ore Geol. Rev.* **2022**, *145*, 104916. [CrossRef]